Faraday Discussions

Accepted Manuscript

This manuscript will be presented and discussed at a forthcoming Faraday Discussion meeting. All delegates can contribute to the discussion which will be included in the final volume.

Register now to attend! Full details of all upcoming meetings: http://rsc.li/fd-upcoming-meetings

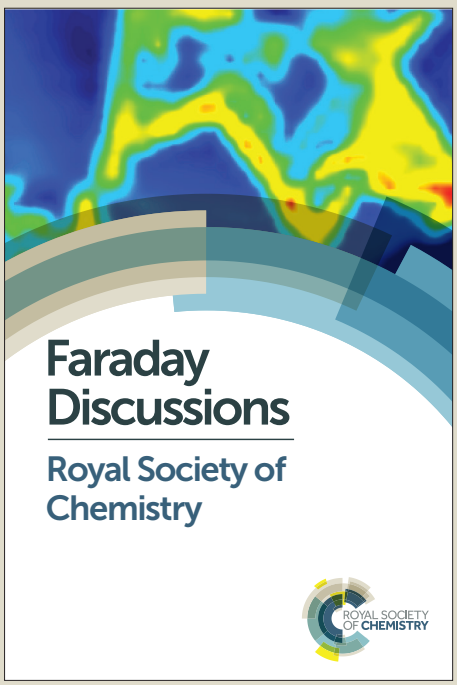

This is an *Accepted Manuscript*, which has been through the Royal Society of Chemistry peer review process and has been accepted for publication.

Accepted Manuscripts are published online shortly after acceptance, before technical editing, formatting and proof reading. Using this free service, authors can make their results available to the community, in citable form, before we publish the edited article. We will replace this *Accepted Manuscript* with the edited and formatted *Advance Article* as soon as it is available.

You can find more information about *Accepted Manuscripts* in the Information for Authors.

Please note that technical editing may introduce minor changes to the text and/or graphics, which may alter content. The journal's standard Terms & Conditions and the Ethical guidelines still apply. In no event shall the Royal Society of Chemistry be held responsible for any errors or omissions in this *Accepted Manuscript* or any consequences arising from the use of any information it contains.

ROYAL SOCIETY OF CHEMISTRY

www.rsc.org/faraday_d

CREATED USING THE RSC LaTeX PCCP ARTICLE TEMPLATE – SEE www.rsc.org/electronicfiles FOR DETAILS
PAPER www. rsc.org/faraday_d | Faraday Discussions

Breaking of a bond: when is it statistical?

Pankaj Yadav,[a] and Srihari Keshavamurthy,*[b]

Received Xth XXXXXXXXXX 20XX, Accepted Xth XXXXXXXXX 20XX
First published on the web Xth XXXXXXXXXX 200X
DOI: 10.1039/c000000x

Unimolecular dissociation dynamics of a model three degree of freedom triatomic molecule is studied in order to understand the mechanisms for deviations from statisticality. Performing a wavelet based time-frequency analysis of the dynamics allows for the dynamics to be followed on the network of nonlinear resonances, also called as the Arnold web. The results indicate that the long lifetime trajectories spend a considerable amount of time trapped near junctions in the web. It is argued that characterizing the dynamics near such junctions might lead to deeper insights into the origins of nonstatistical dynamics.

1 Introduction

A satisfactory answer to the title question is, perhaps surprisingly, still lacking despite several experimental and theoretical studies spanning more than half a century [1]. The term 'statistical' in statistical rate theories refers to a regime where dynamics can be safely ignored in calculating the rate constants and the celebrated Rice-Ramsperger-Kassel-Marcus (RRKM) theory [2–4] is a prime example. At the heart of RRKM theory is the crucial assumption that intramolecular vibrational energy redistribution (IVR) is sufficiently fast as compared to the reaction timescale. Provided this assumption is true, the microcanonical rate constant for a rotationless unimolecular reaction is given by

$$k(E) = \frac{N^{\ddagger}(E)}{2\pi\hbar\rho(E)} \tag{1}$$

where E is the total energy, $N^{\ddagger}(E)$ is the number of states at the transition state with energy less than or equal to E and $\rho(E)$ is the total density of states. In addition, both the population of the unimolecular reactant

$$N(t) = N(0)e^{-k(E)t} \tag{2}$$

and the so called lifetime distribution [5]

$$P(\tau) \equiv -\frac{1}{N(0)}\frac{dN(\tau)}{d\tau} = k(E)e^{-k(E)\tau} \tag{3}$$

[a] *Department of Chemistry, Indian Institute of Technology, Kanpur (U.P.) 208016, India*
[b] *Department of Chemistry, Indian Institute of Technology, Kanpur (U.P.) 208016, India. Fax: +91 512 2597436; Tel: +91 512 2597043; E-mail: srihari@iitk.ac.in*

are expected to decay exponentially. The lifetime distribution above is related to the gap time distribution and enormous efforts have gone into computing and analyzing such distributions. We refer the reader to the paper[6] by Ezra, Waalkens, and Wiggins for a clear exposition of the theory as well as for a detailed historical account.

It is important to note that the exponential decay is a necessary but not sufficient condition and one usually associates the notion of ergodicity with the validity of RRKM. The latter assumption, arising naturally given the classical dynamical origins of RRKM, is a notoriously difficult one to satisfy for Hamiltonians of isolated molecules since they typically exhibit a mixed regular-chaotic phase space even at energies close to the dissociation threshold. Therefore, it is hardly surprising that several studies have identified reactions which are intrinsically non-RRKM in nature[7–14]. Such studies are leading to much needed insights into the dynamics, and hence aiding in identifying novel mechanisms and raising hopes for targeted control of the reaction. Clearly, it is crucial to develop models for reaction rates that eschew the statistical assumption and provide insights into the mechanisms for nonstatistical behaviour.

Deviations from RRKM predictions can be analyzed from two perspectives. The first one[15] associates deviations from the exponential lifetime to the phase space being partitioned into two or more weakly coupled subregions and hence restricted IVR over the entire phase space. Kinetic modeling of such partitioned phase spaces is able to account for the nonexponential $P(\tau)$ in many cases. Nevertheless, highly correlated intramolecular dynamics can lead to the kinetic models being of doubtful utility. At the very least one would have to introduce the correlations into the kinetic scheme - a rather nontrivial task. The second perspective[16,17], coming from the quantum state space model for IVR, has the correlated dynamics already built in and predicts power law scaling[18] for microcanonically averaged quantum survival probabilities. The exponent of the power law determines whether the system is in a regime of restricted or facile IVR. From the state space, and the associated[19,20] local random matrix theory (LRMT), perspective restricted IVR arises due to the state space being partitioned into weakly coupled subregions. The subregions themselves are a result of the various anharmonic resonant couplings leading to a sparse density of locally coupled states. In other words, restricted IVR is a result of the lack of a "percolating cluster" in the state space. Interestingly, a firm connection between the two perspectives is yet to be established. In essence, the issue here is to find the link between the partitioning of the classical phase space and the partitioning of the quantum state space. In other words, what is the quantum analog for the kinetic models? And, at the same time, what is the classical analog for the state space dynamics? Although, answer to the latter question is starting to emerge[21,22], answering the first question and linking the two perspectives together requires a detailed classical-quantum correspondence approach. Arguably, quantum effects like dynamical tunneling[23,24] will somewhat blunt the correspondence. Nevertheless, the failure of the classical-quantum correspondence approach will shed light on the relevance of quantum effects to the observed deviations from statisticality.

In order to address the issues mentioned above, it is crucial to study an appropriate model system from both the perspectives. Although it is desirable to study real molecular systems with large number of degrees of freedom (DOF), a

disadvantage stems from the fact that several different phenomena in such systems can muddle the classical-quantum interpretations. In addition, quantum and classical studies for large systems at required levels of detail present daunting computational challenges. Thus, we choose a minimal model for our study which is still capable of connecting the two perspectives mentioned above. The model (described below) comes from the pioneering studies by Bunker[5,25] on the dissociation rates of model triatomic molecules. Based on a tour de force, at that time, calculation of classical rates and lifetime distribution Bunker provided a list of models that conform to the RRKM theory. A subsequent important paper[26] by Oxtoby and Rice provided insights into the Bunker results using tools, particularly the concept of nonlinear resonance overlap[27], from the field of nonlinear dynamics. However, the work of Oxtoby and Rice replaces the three DOF ($s = 3$) Bunker models with an effective two DOF system. Consequently, as also realized[26] by Oxtoby and Rice, their study cannot reveal novel IVR pathways that are feasible in Bunker's models since there are significant differences between classical phase space transport for $s \geq 3$ systems as compared to the $s = 2$ systems[28]. In this study we undertake a detailed study of the classical dissociation dynamics of a $s = 3$ system, based on one of the Bunker models. We show that the mechanism of IVR and the subsequent dissociation dynamics can only be understood in terms of the network of nonlinear resonances, also known as the Arnold web[29].

2 Model Hamiltonian

The $s = 3$ Hamiltonian of interest is of the form

$$H(\mathbf{p},\mathbf{q}) = \sum_{k=1}^{3}\left[\frac{1}{2}G^0_{kk}p_k^2 + V_k(q_k)\right] + \sum_{k<l=1}^{3} G^0_{kl}p_k p_l \tag{4}$$

with $k = 1,2$ and $k = 3$ modeling the anharmonic stretching modes and a bending mode respectively of a nonlinear triatomic molecule. The potential functions $V_k(q_k)$ are chosen to be Morse oscillators for the stretching modes

$$V_k(q_k) = D_k\left(1 - e^{-a_k(q_k - q_k^0)}\right)^2, \tag{5}$$

and as a harmonic oscillator for the bending mode

$$V_3(q_3) = \frac{1}{2G^0_{33}}\omega_3^2(q_3 - q_3^0)^2. \tag{6}$$

The various Hamiltonian parameters are determined such that $D_1 = D_2 = 24$ kcal mol^{-1} with the resulting mode harmonic frequencies being $\nu_1 = 1112$ cm^{-1}, $\nu_2 = 1040$ cm^{-1}, and $\nu_3 = 632$ cm^{-1}, corresponding to Bunker's model 6 for ozone[5]. However, eq. 4 is a simplified version of the one used by Bunker in that the G-matrix elements have been replaced with their equilibrium values. The simplified version affords a couple of advantages. First, the action-angle representation of eq. 4 is easily obtained and allows one to extract the strengths of the various anharmonic resonances. Second, gauging the influence of the bending

mode on the dissociation dynamics is straightforward without losing the essential three DOF nature of the system. Thus, setting $G^0_{13} = G^0_{23} = 0$ yields a $(2+1)$ DOF system with the bend mode decoupled from the coupled stretching modes subsystem. Note that the subsystem itself has been the subject of detailed dynamical studies[30] starting with the classic work[31] of Thiele and Wilson.‡ Hence, the minimal model of eq. 4 is ideally suited for highlighting the central issues of interest to the present work.

2.1 Action-angle representation: location and strengths of the resonances

The Hamiltonian in eq. 4 can be conveniently transformed to the action-angle $(\boldsymbol{J},\boldsymbol{\theta})$ representation since the exact action-angle variables for both the Morse[32] and the harmonic oscillators are known. The resulting Hamiltonian $H(\boldsymbol{J},\boldsymbol{\theta}) \equiv H_0(\boldsymbol{J}) + V(\boldsymbol{J},\boldsymbol{\theta})$ has a integrable zeroth-order part

$$H_0(\mathbf{J}) = \omega_3 J_3 + \sum_{k=1,2} \omega_k \left[J_k - \frac{\omega_k}{4D_k} J_k^2 \right], \tag{7}$$

and the coupling term which can be explicitly written as a Fourier expansion

$$\begin{aligned} V(\boldsymbol{J},\boldsymbol{\theta}) &= \sum_{\alpha,\beta=1}^{\infty} v_{\alpha\beta}(J_1,J_2)\left[\cos(\alpha\theta_1 - \beta\theta_2) - \cos(\alpha\theta_1 + \beta\theta_2)\right] \\ &+ \sum_{k=1,2}\sum_{\alpha=1}^{\infty} u_{\alpha}(J_k,J_3)\left[\sin(\alpha\theta_k - \theta_3) + \sin(\alpha\theta_k + \theta_3)\right]. \end{aligned} \tag{8}$$

In the above, the main terms responsible for IVR and dissociation are the various resonances§ of the form $\cos(\alpha\theta_i - \beta\theta_j)$ or $\sin(\alpha\theta_i - \beta\theta_j)$ with strengths $v_{\alpha\beta}(\mathbf{J})$ or $u_\alpha(\mathbf{J})$. A specific resonance occurs when

$$\frac{d}{dt}(\alpha\theta_i - \beta\theta_j) = \alpha\dot{\theta}_i - \beta\dot{\theta}_j \equiv \alpha\Omega_i - \beta\Omega_j = 0, \tag{9}$$

with Ω_i being the nonlinear frequency associated with the i^{th} mode. The above resonance condition, satisfied for certain resonant action values $\mathbf{J}^r$, can be compactly written as $\mathbf{r}\cdot\boldsymbol{\Omega}^r = 0$ with $\mathbf{r} = (\alpha,-\beta)$ and $\boldsymbol{\Omega}^r \equiv \boldsymbol{\Omega}(\boldsymbol{J}^r) = (\Omega^r_i,\Omega^r_j)$. The zone of influence of a resonance scales as the square root of the strength of the resonance which decrease rapidly with the so called order of a resonance $O = |\alpha| + |\beta|$.

The role of such resonances in the dissociation dynamics comes from the Chirikov overlap criterion[27] whereby overlap of various resonances lead to stochasticity in the phase space and hence, presumably, rapid IVR followed by dissociation of the critical bond. Oxtoby and Rice hypothesized[26] that the validity of RRKM at a specific energy is linked to the extensive resonance overlap that occurs at that energy. However, as mentioned in the introduction, the hypothesis has a very strong two DOF flavor to it and the key assumption of the existence of isolated resonance zones needs to be scrutinized carefully.

‡ It is interesting that the referee to this classic work did point out the "danger of generalizing from triatomic to complex polyatomic molecules". The referee's concerns are true even regarding generalization from a linear triatomic (2 DOF) to a bent triatomic (3 DOF).

§ Quantum analogs of the classical nonlinear resonances are precisely the Fermi resonances.

2.2 Two versus three DOF: isolated resonances versus the Arnold web

The key difference between two and three DOF classical dynamics for our model Hamiltonian can be illustrated rather dramatically by first considering the dynamics with the bending mode decoupled from the stretching modes. Moreover, the total energy of the 2 DOF stretching subsystem is fixed at 15 kcal mol^{-1}, far below the dissociation energy of the oscillators. In Fig. 1A all possible resonances up to order five are shown within the Chririkov approximation for the subsystem. Clearly, at 15 kcal mol^{-1} there is no extensive overlap of the resonances and one does not expect any dissociation to occur. The corresponding phase space in Fig. 1B qualitatively agrees with the state space picture in Fig. 1A and shows the existence of the $1:1$ resonance along with a substantial degree of chaos. As expected, none of the four initial conditions shown in Fig. 1B dissociate. In this 2 DOF case, initial conditions inside the $1:1$ island are trapped forever classically.

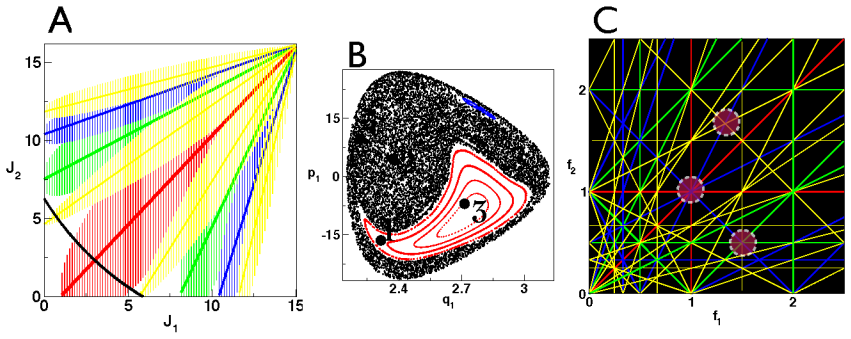

Fig. 1 (A) Resonances up to a maximum order of five and their widths in the (J_1, J_2) state space for the coupled Morse stretch subsystem. The black line is the $H_0(J_1, J_2) = 15$ kcal mol^{-1} isoenergy line. (B) Poincaré surface of section (q_1, p_1) at $q_2 = q_2^0$ for the subsystem at 15 kcal mol^{-1} shows a large $1:1$ resonance zone embedded in the chaotic sea. Black dots are specific initial conditions of interest. (C) Arnold web represented in the frequency ratio space $(f_1, f_2) = (\Omega_1/\Omega_3, \Omega_2/\Omega_3)$ showing the possible resonances (without the widths) up to order five. A few example resonance junctions are highlighted with circles. In A and C the resonances are color coded with red, green, blue and yellow representing orders of $2, 3, 4$,and 5 respectively.

The above brief description gives the essence of the IVR dynamics in 2 DOF and emphasizes a crucial feature - at a given energy, trapping in isolated resonance zones will lead to non-RRKM behavior. However, adding the third bending DOF to the subsystem leads to a qualitative and fundamental change of this picture. Addition of the third mode, and hence for the full Hamiltonian in eq. 4, the general resonance condition involves three frequencies and can be written down as

$$\alpha\Omega_1 + \beta\Omega_2 + \gamma\Omega_3 = 0. \tag{10}$$

The above condition represents a resonance plane in the full (J_1, J_2, J_3) state space. These resonance planes intersect the constant energy surface in resonance lines. The collection of all such resonance lines on a given energy surface is known as the Arnold web[29]. The crucial difference between two and three DOF is now apparent; in contrast to the former case, resonances in the latter case form

an intricate network and are not isolated on the energy surface. In Fig. 1C we show the Arnold web in the so called frequency ratio space (FRS)[33] wherein eq. 10 can be expressed in terms of $(f_1, f_2) = (\Omega_1/\Omega_3, \Omega_2/\Omega_3)$ as

$$f_2 = -\frac{\alpha}{\beta} f_1 - \frac{\gamma}{\beta} \tag{11}$$

A distinct feature of systems with DOF > 2 is the occurrence of junctions wherein several independent resonances on the energy surface intersect. For example, Fig. 1C shows a junction at $(f_1, f_2) = (1,1)$ formed by two independent resonances $(\alpha, \beta, \gamma) = (1, 0, -1)$ and $(0, 1, -1)$. The number of independent resonances forming the junction determine the multiplicity of the junction. Thus, $(1,1)$ in Fig. 1C is a multiplicity two junction. Two important points are worth noting. First, an infinity of resonances of various orders emanate from a junction. Second, large scale transport can occur on the Arnold web with the junctions playing a central role in the dynamics. Thus, although a trajectory can be indefinitely trapped in the 1 : 1 zone in Figs. 1A and B, coupling in the bending mode can detrap the trajectory. Consequently, arguments based on the Chirikov overlap criterion alone are not sufficient to predict the statisticality of the bond breaking process. Understanding the dynamics from the Arnold web perspective is necessary. Is it possible, however, to quantify the extent of non-RRKM behaviour from such a perspective? What role do the junctions in Fig. 1C play in the dissociation dynamics of our model Hamiltonian? Is there a connection, both qualitative and quantitative, between the lifetime distribution of eq. 3 and the dynamics on the FRS? In the next few sections we attempt to answer these questions.

3 Dissociation dynamics: role of the resonance junctions

We start this section by noting that the initial conditions shown in Fig. 1B, corresponding to a total energy of 25 kcal mol^{-1} with 15 kcal mol^{-1} in the subsystem, do not dissociate. However, upon coupling the bend mode all four initial conditions do lead to dissociation. Interestingly, trajectories 1 and 3, starting from a regular region of the subsystem phase space, have lifetimes of about 1.4 ps and 8.6 ps respectively. On the other hand, trajectories 2 and 4 start from the chaotic region of the phase space and have lifetimes of about 2.8 ps and 18.8 ps respectively. Clearly, trajectories 3 and 4 belong to the non-RRKM class. This observation immediately shows that any attempt to *a priori* associate trajectories originating from chaotic regions in the subsystem phase space with RRKM behaviour is incorrect. Nevertheless, it is crucial to understand the mechanism which leads to such long lifetime trajectories. As argued in the previous section, detailed insights in this regard are expected[33] to come from the dynamics in the FRS. However, this requires extracting the mode frequencies as a function of time and several studies have shown[21,22,34–39] that a wavelet based time-frequency analysis[34,35] is ideally suited for this purpose. In particular, for irregular trajectories, the variations of the nonlinear frequencies with time is capable of providing deep insights into the transport occurring in the multidimensional phase space. Note that the static Arnold web in Fig. 1C only indicates the possible resonances that can play a role and it is absolutely important to extract the time dependent

frequencies in order to identify the key resonances and the dynamically relevant regions of the web. In this sense, Fig. 1C can be thought of as a template to understand the dynamics in the FRS.

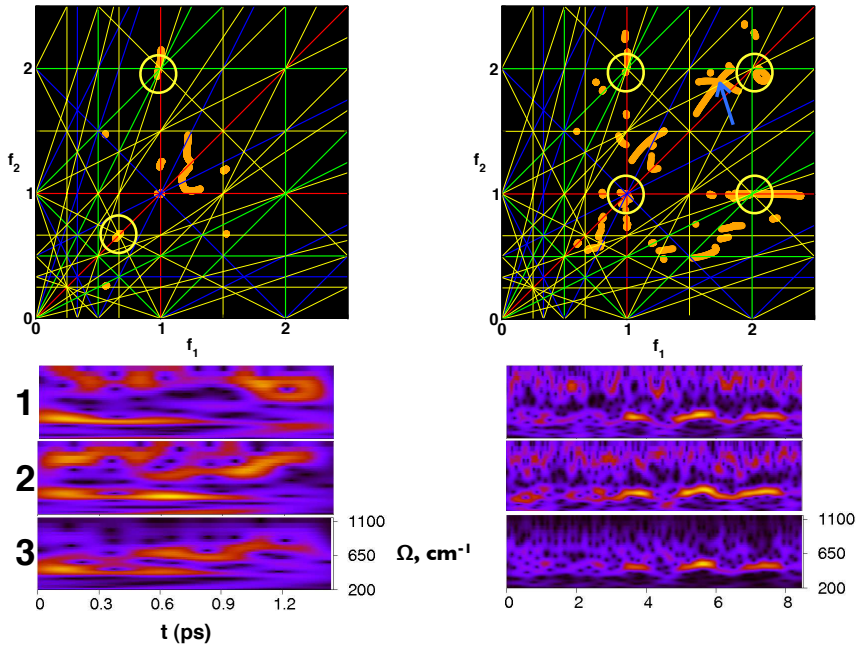

Fig. 2 The top left and right panels show the evolution of the dynamics on the frequency ratio space for initial conditions 1 and 3 shown in Fig. 1B. Circled regions highlight the resonance junctions near which significant activity is observed. The corresponding full scalograms (modes indicated) for initial condition 1 and 3 are shown in the bottom left and right multipanels respectively. Scalograms for each case have the same axis range as shown for mode 3. In the top tight FRS, the blue arrow indicates high density possibly near junctions of much higher order than shown in the plot. Total energy at 25 kcal mol^{-1} for both trajectories.

We give here a brief description of the time-frequency analysis since details can be found in previous works[22,34,35]. The time series $z_k(t) = q_k(t) + ip_k(t)$, obtained from the dynamics, for the three modes $(k = 1,2,3)$ are subjected to a continuous wavelet transform[34]

$$L_\psi z_k(a,b) = a^{-1/2} \int_{-\infty}^{\infty} z_k(t) \psi^* \left(\frac{t-b}{a} \right) dt, \tag{12}$$

for $a > 0$ and b real and

$$\psi(t) = \frac{1}{\sigma\sqrt{2\pi}} e^{2\pi i \lambda t} e^{-t^2/2\sigma^2}, \tag{13}$$

with $\lambda = 1$ and $\sigma = 2$ is the Morlet-Grossman wavelet. Equation 12 gives the local frequency of $z_k(t)$ over a small interval of time around $t = b$ and inverse of the scale factor a is proportional to the frequency. There are two ways of analyzing the transform. First is to extract the dominant frequency at a given

time by computing the maximum of the modulus of the wavelet transform of $\mathbf{z}(t)$ *i.e.,* $\max_a |L_\psi \mathbf{z}(a,b)|$. The ratios of the dominant frequencies can then be used to analyze the dynamics in the FRS. A second more comprehensive way[35] is to compute the full scalogram $|L_\psi z_k(a,b)|^2$ to look at the ridge maxima and dominant frequency variations over time.

The results of our computation are summarized in Fig. 2 for two of the initial conditions labeled 1 and 3 in the susbsytem phase space shown in Fig. 1B. The total energy is fixed at 25 kcal mol^{-1}, just above the dissociation energy of the Morse oscillators. Breaking of either mode 1 or mode 2 was identified as dissociation in accordance with the criteria used by Bunker. Clearly, Fig. 2 shows a distinct difference between the FRS dynamics of the two trajectories. The short lifetime trajectory visits very few of the numerous resonance junctions whereas trajectory 3 with $\tau \approx 8.6$ ps spends an appreciable amount of time near $(2,1)$, $(2,2)$, and $(1,2)$ junctions. Moreover, as shown by a blue arrow in Fig. 2 (upper right panel), there are indications that the dynamics is influenced by resonance junctions formed by resonances of orders higher then five. Note that the FRS range shown in Fig. 2 is energetically accessible and hence lack of density in certain regions suggest the existence of dynamical barriers.

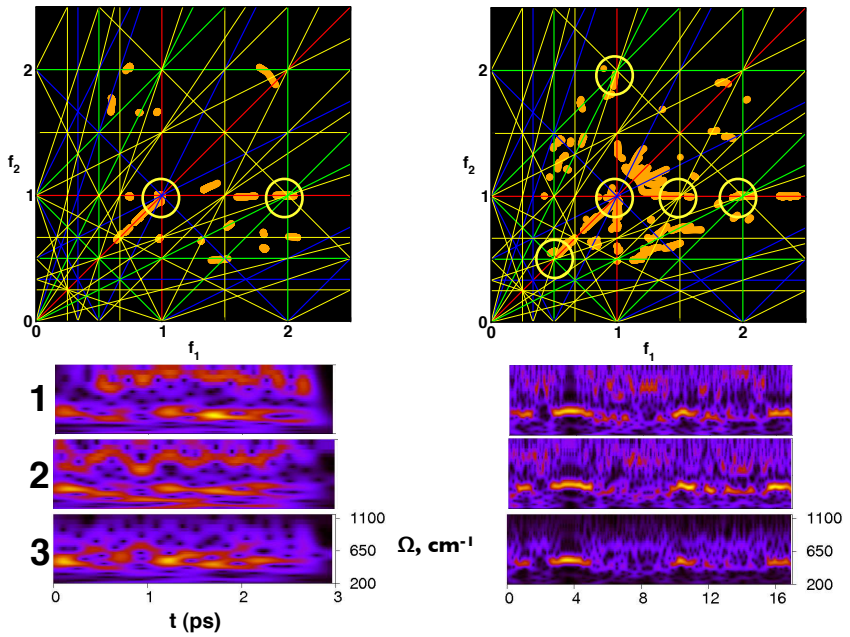

Fig. 3 Same as in Fig. 2 for initial conditions 2 and 4 respectively. Total energy at 25 kcal mol^{-1} for both trajectories.

In Fig. 3 we summarize the FRS dynamics for the initial conditions 2 and 4 as shown in Fig. 1C along with the scalograms. Note that both trajectories start in the chaotic part of the subsystem phase space and yet their lifetimes differ by nearly a factor of six. The reasons for this difference becomes clear from the FRS shown in Fig. 3 wherein the long lifetime trajectory is seen accessing several resonance junctions. Apart from the main $(1,1)$ junction, seen in the pre-

vious cases as well, the trajectory is clearly spending sufficient amount of time near the $(3/2,1)$, $(4/3,2/3)$, and the $(1/2,1/2)$ junctions. The main point here is that the FRS shows significant anisotropy despite the considerable delocalization with the anisotropy originating from the trajectory "sticking" around the various junctions. In contrast, the shorter lifetime trajectory is accessing far fewer junctions with almost no density near junctions formed by high order resonances such as the $(4/3,2/3)$ junction.

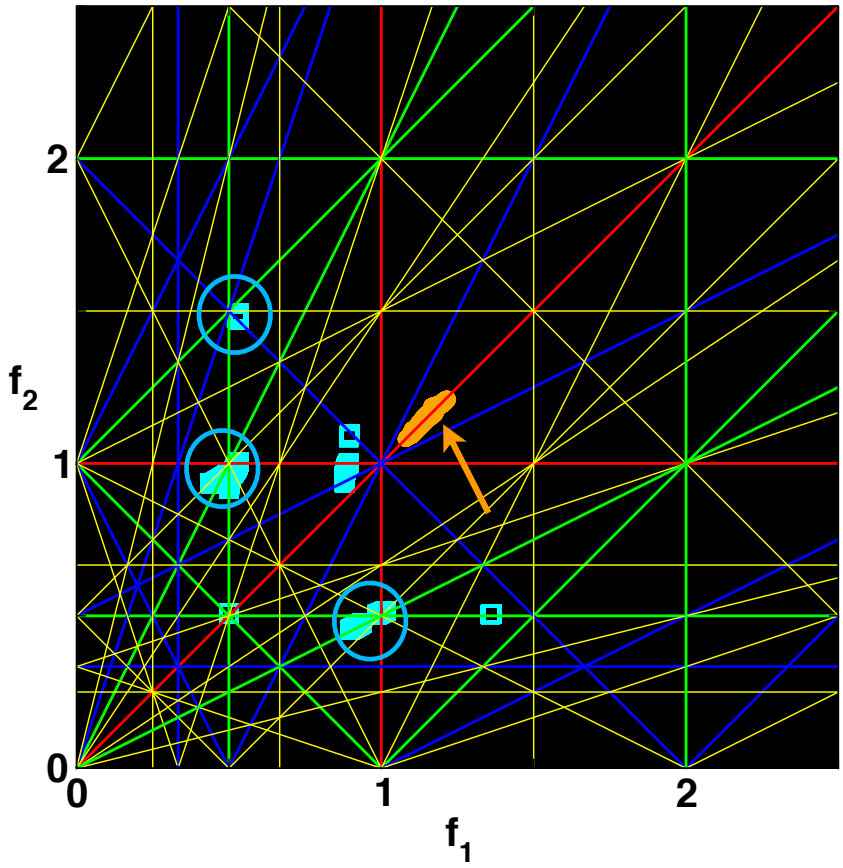

Fig. 4 FRS dynamics for two specific trajectories. The first one (orange) corresponds to trajectory 3 in Fig. 1C with the bend mode decoupled and total energy of 25 kcal mol^{-1}. The dynamics is clearly localized (arrow) around the 1 : 1 resonance. The second trajectory (cyan) is at a total energy of 40 kcal mol^{-1} and has a lifetime of $\sim$ 1.2 ps. Trapping near resonance junctions are highlighted with circles.

As a contrast to the cases discussed above, Fig. 4 shows the FRS dynamics for two trajectories. The first one is the trajectory 3 as before except that the coupling of the bend mode to the stretches has been turned off. As expected from the surface of section shown in Fig. 1B, and in strong contrast to Fig. 2 (top right panel), the trajectory is localized in the 1 : 1 stretch-stretch resonance for all time. The second case pertains to a trajectory with a total energy of 40 kcal

mol^{-1} which is far above the dissociation energy. The lifetime of this particular trajectory is about 1.2 ps and is relatively large compared to the typical lifetimes for most dissociating trajectories at this energy. The reason for this becomes clear from Fig. 4 wherein trapping near $(1/2, 3/2)$, $(1/2, 1)$, and $(1, 1/2)$ junctions can be seen.

The results shown in this section clearly indicate a strong correlation between long lifetime trajectories and enhanced density around various multiplicity two resonance junctions. Such junctions invariably involve the bending mode and the scalograms show that the bending modes actively participate in the IVR even at early times. We stress that the examples shown are representative and several other trajectories exhibit very similar characteristics in the FRS. It is also worth pointing out that significant differences can be seen between Fig. 2 and Fig. 3 corresponding to the dynamics of the two long lifetime trajectories. Note that existence of such junctions and their influence on the dissociation dynamics is a genuine three DOF feature and cannot be uncovered by effective models which have lesser than three DOF.

4 Discussion and open problems

The results shown in this work provide an important clue to the title question. Dissociating trajectories which have very small sojourn times near the resonance junctions are expected to behave statistically. This observation is reminiscent of an earlier work[40] by Hamilton and Brumer in that trapping near junctions lead to long time dynamical correlations and hence would violate the so called zero relevance condition. The emphasis of this work on junctions is also in line with the early observations[41] of Engel and Levine who argued that large scale IVR requires the participation of at least three modes. Interestingly, our results indicate that the junctions might slow down IVR just enough to violate statisticality. Studies by Bach, Hostettler and Chen on the unimolecular dissociation of ethyl radical, using the approach of time-frequency analysis, hint towards episodes of regularity in the dynamics even at energies far above the dissociation threshold[36]. It is not known whether there is any role of junctions in their studies.

This work is inspired by the seminal work of Martens, Davis, and Ezra[33] where the first attempts to use the FRS to understand the IVR dynamics of planar OCS were undertaken. More recently, Paskauskas, Chandre, and Uzer provided[42] a detailed study of the phase space of planar OCS and identified one possible mechanism of trapping and escape involving a class of two-dimensional invariant tori. The results presented in this work point towards a connection between these studies which, however, is not yet established. Of course, the clue regarding links between non-RRKM and trapping near junctions raises several questions and we list a few of them below for further work and discussions.

1. Which features of the junction determine the extent of trapping of a trajectory? This requires detailed studies comparing, for instance, the nature of the dynamics near a junction involving a strong low order resonance and a weak high order resonance with dynamics near a junction formed by two high order resonances. Although methods do exist[43–46] to study such problems, it remains to be seen if quantitative measures for deviations from

RRKM can be obtained using such approaches.

2. In this study of a three DOF system, one can only have junctions with multiplicity two. In higher DOF systems one can have junctions of different multiplicities and such a scenario would be generic to many realistic molecular systems. However, not much is known about the dynamics near junctions with less then maximal multiplicity in such cases. A puzzling observation here is worth mentioning. For systems with very large number of DOF it appears that the Arnold web will be densely populated with resonance junctions. In turn, given that trajectories can get trapped near junctions, this implies that nonstatisticality may be the rule rather than exception.

3. Recent work[47] suggests that local dynamical traps near junctions can slow down the quantum IVR dynamics. However, the issue of whether quantum dynamical tunneling? can also help in escaping from the trap is largely unexplored. If dynamical tunneling dominates, as is expected[48] for polyatomic systems with a large density of states, then that might resolve the puzzle mentioned above.

4. Finally, is it possible to relate the number of dominant junctions with the number of partitions in the kinetic schemes mentioned earlier? Clearly, in order to establish such a connection one would have to relate the trapping or residence times[46] near the junctions with the weighting factors λ_i in the multi exponential fit[15] $P(\tau) = \sum_i \lambda_i \exp(-k_i\tau)$ to the lifetime distribution. Since several studies have already established the close correspondence between the FRS and the quantum state space models of IVR, progress in this regard will help in relating the two perspectives mentioned in the introduction.

Acknowledgements

PY gratefully acknowledges the University Grants Commission of India for a graduate fellowship.

References

1 W. L. Hase and T. Baer, *Unimolecular Reaction Dynamics - Theory and Experiment*, Oxford University Press, New York, 1st edn, 1996.
2 O. K. Rice and H. C. Ramsperger, *J. Am. Chem. Soc.*, 1927, **49**, 1617–1629.
3 L. S. Kassel, *J. Phys. Chem.*, 1928, **32**, 225–242.
4 R. A. Marcus, *J. Am. Chem. Soc.*, 1952, **20**, 359–364.
5 D. L. Bunker, *J. Chem. Phys.*, 1962, **37**, 393–403.
6 G. S. Ezra, H. Waalkens and S. Wiggins, *J. Chem. Phys.*, 2009, **130**, 164118.
7 U. Lourderaj and W. L. Hase, *J. Phys. Chem. A*, 2009, **113**, 2236–2253.
8 J. Rehbein and B. K. Carpenter, *Phys. Chem. Chem. Phys.*, 2011, **13**, 20906–20922.
9 M. Paranjothy, R. Sun, A. K. Paul and W. L. Hase, *Z. Phys. Chem.*, 2013, **227**, 1361–1379.
10 R. A. Marcus, *Proc. Natl. Acad. Sci. (USA)*, 2013, **110**, 17703–17707.
11 M. Kryvohuz and R. A. Marcus, *J. Chem. Phys.*, 2010, **132**, 224304.
12 M. Berblinger and C. Schlier, *J. Chem. Phys.*, 1994, **101**, 4750–4758.
13 B. C. Dian, G. E. Brown, K. O. Douglass and B. H. Pate, *Science*, 2008, **320**, 924–928.

14 B. C. Dian, G. G. Brown, K. O. Douglass, F. S. Rees, J. E. Johns, P. Nair, R. D. Suenram and B. H. Pate, *Proc. Natl. Acad. Sci. (USA)*, 2008, **105**, 12696–12700.
15 R. A. Marcus, W. L. Hase and K. N. Swamy, *J. Phys. Chem.*, 1984, **88**, 6717–6720.
16 M. Gruebele, *Adv. Chem. Phys.*, 2000, **114**, 193–261.
17 M. Gruebele and P. G. Wolynes, *Acc. Chem. Res.*, 2004, **37**, 261–267.
18 S. Schofield and P. G. Wolynes, *J. Chem. Phys.*, 1993, **98**, 1123–1131.
19 D. E. Logan and P. G. Wolynes, *J. Chem. Phys.*, 1990, **93**, 4994–5012.
20 D. M. Leitner and P. G. Wolynes, *J. Phys. Chem. A*, 1997, **101**, 541–548.
21 A. Semparithi and S. Keshavamurthy, *J. Chem. Phys.*, 2006, **125**, 141101.
22 S. Keshavamurthy, *Adv. Chem. Phys.*, 2013, **153**, 43–110.
23 M. J. Davis and E. J. Heller, *J. Chem. Phys.*, 1981, **75**, 246–254.
24 S. Keshavamurthy, *Int. Rev. Phys. Chem.*, 2007, **26**, 521–584.
25 D. L. Bunker, *J. Chem. Phys.*, 1964, **40**, 1946–1957.
26 D. W. Oxtoby and S. A. Rice, *J. Chem. Phys.*, 1976, **65**, 1676–1683.
27 B. V. Chirikov, *Phys. Rep.*, 1979, **52**, 263–379.
28 S. Wiggins, *Chaotic Transport in Dynamical Systems*, Springer-Verlag, New York, 1st edn, 1992.
29 A. L. Lichtenberg and M. A. Lieberman, *Regular and Chaotic Dynamics*, Springer, New York, 2nd edn, 1992.
30 E. Thiele, *J. Chem. Phys.*, 1963, **38**, 1959–1966.
31 E. Thiele and D. J. Wilson, *J. Chem. Phys.*, 1961, **35**, 1256–1263.
32 R. B. Shirts, *J. Phys. Chem.*, 1987, **91**, 2258–2267.
33 C. C. Martens, M. J. Davis and G. S. Ezra, *Chem. Phys. Lett.*, 1987, **142**, 519–528.
34 L. V. Vela-Arevalo and S. Wiggins, *Int. J. Bifur. Chaos.*, 2001, **11**, 1359–1380.
35 C. Chandre, S. Wiggins and T. Uzer, *Physica D*, 2003, **181**, 171–196.
36 A. Bach, J. M. Hostettler and P. Chen, *J. Chem. Phys.*, 2005, **123**, 021101.
37 A. Shojiguchi, C. B. Li, T. Komatsuzaki and M. Toda, *Phys. Rev. E*, 2007, **76**, 056205.
38 A. Sethi and S. Keshavamurthy, *Mol. Phys.*, 2012, **110**, 717–727.
39 J. C. Losada, R. M. Benito and F. Borondo, *Eur. Phys. J. Spec. Top.*, 2008, **165**, 183–193.
40 I. Hamilton and P. Brumer, *J. Chem. Phys.*, 1985, **82**, 1937–1946.
41 Y. M. Engel and R. D. Levine, *Chem. Phys. Lett.*, 1989, **164**, 270–278.
42 R. Paskauskas, C. Chandre and T. Uzer, *J. Chem. Phys.*, 2009, **130**, 164105.
43 C. Efthymiopoulous, *Celest. Mech. Dyn. Astr.*, 2008, **102**, 49–68.
44 M. Guzzo and E. Lega, *Chaos*, 2013, **23**, 023124.
45 G. Haller, *Phys. Lett. A*, 1995, **200**, 34–42.
46 S. Honjo and K. Kaneko, *Adv. Chem. Phys.*, 2005, **130B**, 437–463.
47 P. Manikandan and S. Keshavamurthy, *Proc. Natl. Acad. Sci. (USA)*, 2014, **111**, 14354–14359.
48 D. M. Leitner and P. G. Wolynes, *Phys. Rev. Lett.*, 1996, **76**, 216–219.

